



An Iterative Numerical Approach to Evaluate the Variable Friction Coefficient of Steel AMS5643 Using Ring Compression Tests

Jacob Hatherell, Grant Dennis, Will Curry, Arnaud Marmier & Jason Matthews

To cite this article: Jacob Hatherell, Grant Dennis, Will Curry, Arnaud Marmier & Jason Matthews (2024) An Iterative Numerical Approach to Evaluate the Variable Friction Coefficient of Steel AMS5643 Using Ring Compression Tests, Tribology Transactions, 67:1, 15-21, DOI: [10.1080/10402004.2023.2284347](https://doi.org/10.1080/10402004.2023.2284347)

To link to this article: <https://doi.org/10.1080/10402004.2023.2284347>



© 2023 The Author(s). Published with license by Taylor & Francis Group, LLC.



Published online: 15 Dec 2023.



Submit your article to this journal [↗](#)



Article views: 263




View related articles [↗](#)



View Crossmark data [↗](#)

An Iterative Numerical Approach to Evaluate the Variable Friction Coefficient of Steel AMS5643 Using Ring Compression Tests

Jacob Hatherell^a, Grant Dennis^b, Will Curry^c, Arnaud Marmier^a, and Jason Matthews^a 

^aEngineering Design and Mathematics, University of the West of England, Bristol, United Kingdom; ^bEngineering & Business Development, SKF Group, Clevedon, United Kingdom; ^cProduct Engineering, SKF Group, Clevedon, United Kingdom

ABSTRACT

The coefficient of friction is an important variable that must be defined to allow the accurate prediction of the forming geometry and stresses involved in metal forming processes. Literature reports have shown that the coefficient of friction does not remain constant with respect to variables including but not limited to contact pressure, sliding speed, surface roughness, and surface morphology. Ring compression tests provide a simple and efficient process by which to measure the variable coefficient of friction present in the bulk-metal process; however, the conventional interpolating method can result in a poor evaluation of the evolution of friction, especially if the coefficient of friction changes significantly during a test. In this article, a novel approach to evaluate the relationship between the coefficient of friction and contact pressure is outlined using friction calibration charts generated via iterative computation models and ring compression tests. This relationship can be programmed into a computational model to allow for the coefficient of friction to behave as a dynamic variable. This approach improves on the prediction of the computational model when compared to conventional interpolation methods.

ARTICLE HISTORY

Received 13 July 2022
Accepted 10 November 2023

KEYWORDS

Friction; cold forming; ring compression test; computation modeling

Introduction

The coefficient of friction between the workpiece and tooling must be correctly defined to be able to accurately predict the stresses, forming load, energy consumption, and final part geometry in a metal forming process. However, it is inherently difficult to precisely quantify even within a simple static problem due to the number of factors that can influence the coefficient of friction (1, 2). Some of these influencing factors include, but are not limited to, surface roughness and morphology (3–7), contact pressure (8–10), lubricants (11), workpiece and die material combinations, and temperature (12, 14).

While many of these parameters can be considered constant during a given metal forming process, parameters such as surface roughness dynamically change throughout the process due to both the high contact pressures and plastic deformation present, which can result in a variable coefficient of friction. The current state of the art for computational modelling is not able to capture or model the behavior of many of these dynamic parameters. Therefore, it is not possible to define a variable coefficient of friction within a computation modeling environment as a function of a parameter such as surface roughness or morphology. One of the few parameters that can be used to define a variable coefficient of friction within a computational model is

the contact pressure between two mating surfaces, which can be obtained from a ring compression test.

Building off the work of Kunugi (15), Male and Cockcroft (16) published a standard methodology for determining the coefficient of friction through the use of a ring compression test (Fig. 1). The test consists of a ring compressed axially between two flat and parallel compression platens, such that the material undergoes plastic deformation. If the interface between the specimen and dies is of sufficiently low friction (assuming isotropic material properties, perfect-plastic behavior, and homogeneous deformation), then the inner diameter of the ring will expand together with the outer diameter. As the friction increases, sticking will occur at the interface, which resists the outward flow of material, causing the specimen to bulge at the mid-plane (barreling). Once the friction coefficient reaches a critical value it becomes favorable for material to flow inward and results in the reduction of the inner diameter. The coefficient of friction is evaluated by interpolating between the relationship of the inner diameter and height of the specimen against analytically derived friction calibration curves (FCCs) at constant coefficients of friction. This results in all the potential influencing factors on the coefficient of friction being reduced to a single parameter that is the contact pressure between the workpiece and dies.

CONTACT Jacob Hatherell  Jacob2.Hatherell@live.uwe.ac.uk
Review led by M. Marinack.

© 2023 The Author(s). Published with license by Taylor & Francis Group, LLC.

This is an Open Access article distributed under the terms of the Creative Commons Attribution-NonCommercial-NoDerivatives License (<http://creativecommons.org/licenses/by-nc-nd/4.0/>), which permits non-commercial re-use, distribution, and reproduction in any medium, provided the original work is properly cited, and is not altered, transformed, or built upon in any way. The terms on which this article has been published allow the posting of the Accepted Manuscript in a repository by the author(s) or with their consent.

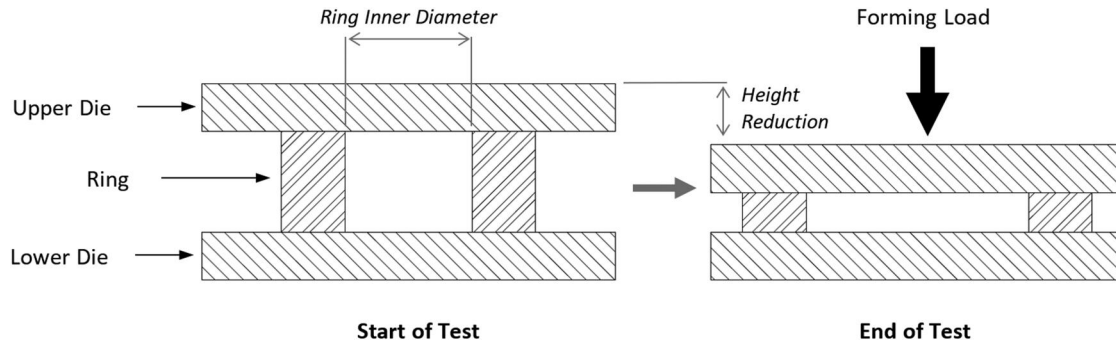


Figure 1. Ring compression test schematic.

The use of computational modeling to numerically derive the FCCs (10, 11, 14, 17, 19) has allowed for the incorporation of material behaviors not possible via analytical methods, such as strain rate, strain hardening, and nonuniform contact pressures. While the interpolation method for determining the coefficient of friction from a ring compression test is an efficient process, as will be later investigated, interpolating the coefficient of friction between FCCs can result in a poor evaluation of the evolution of friction with respect to contact pressure, especially if the coefficient of friction is rapidly changing.

Despite evidence indicating that the coefficient of friction (under the correct conditions) can vary with respect to contact pressure (10, 21–23), it is still common practice for the coefficient of friction to be quoted and modeled as a static value (17, 24–27). The complex nature of friction and the comparably high cost required to investigate these phenomena give little incentive to conduct research or change industrial practices. However, with respect to bulk-metal forming, one of the largest factors leading to a loss in production is excessive die wear or failure whereby friction is the leading contributing factor (28), highlighting the importance of understanding this phenomenon. Recent research has begun to see the integration of a variable friction coefficient into computational models with the aim of improving the accuracy of both sheet (26) and bulk-metal forming (10, 19, 30). This is an active area of research and a continuing area of debate as to how to best implement variable friction coefficients into numerical and analytical models.

In this article, a new method for determining the pressure–friction relationship is presented where ring compression tests are analyzed with an iterative computational model. This is compared to the conventional approach of interpolating experimental data against FCCs. For this study, the two methods are referred to as the “iterative FCC” and “FCC interpolation.” This research was in support of a wider study of work into the bulk-metal cold-forming process of staking, which is widely used in the aerospace sector for the manufacture and assembly of spherical-plain bearings and rod-end links (31). This manufacturing process is characterized as a single-strike operation, similar to wire crimping and sheet metal pressing. Therefore, the material investigated in this research was steel AMS5643, with all testing conducted at room temperature, to best replicate the

Table 1. Chemical composition of AMS5643.

| Element | C | Mn | P | S | Si | Cr | Ni | Cu | Mo | Nb |
|-------------|------|----|------|------|----|------|----|----|-----|------|
| Content (%) | 0.07 | 1 | 0.04 | 0.03 | 1 | 17.5 | 5 | 5 | 0.5 | 0.45 |

conditions experienced in the manufacturing of spherical-plain bearings.

Methodology

Test specimens

AMS5643 (H1150 condition) is a high-strength, corrosion-resistant steel used extensively within the aerospace industry. The chemical composition is given in Table 1.

There is no consensus on the most suitable specimen dimensions for a ring compression test; however, it has been shown that increasing the inner diameter can lead to an increase in measurement accuracy (32). If the inner diameter is increased too much, then the ring risks buckling during deformation due to the thinner wall thickness. This can be compensated for by increasing the outer diameter in kind, but this will have the undesired effect of increasing the required forming load. The most commonly used ratio of outer diameter to inner diameter to height (OD:ID:H) used is 6:3:2 (10,18,19) with an inner diameter of 9.53 mm; therefore, these dimensions were chosen for this study (Fig. 2). To maintain consistency between test specimens, the surface roughness (Ra) was machined to a finish of 1.6 μm and verified using a contact-type roughness meter.

Experiment setup

In total, 20 specimens were produced to ensure that an adequate number of data points could be acquired to ensure statistically valid results. Molybdenum disulfide lubricant (G-n Plus) was applied to each face of both the specimens and to the compression platens. Tests were conducted using a 640-kN, four-column press with tungsten carbide plates (Grade YG15) inserted into the compression platens to function as the upper and lower die surfaces.

The load profile of the press was set to 15 kN and increased in increments of 5 kN to reduce the height of the specimens in even increments from approximately 10 to

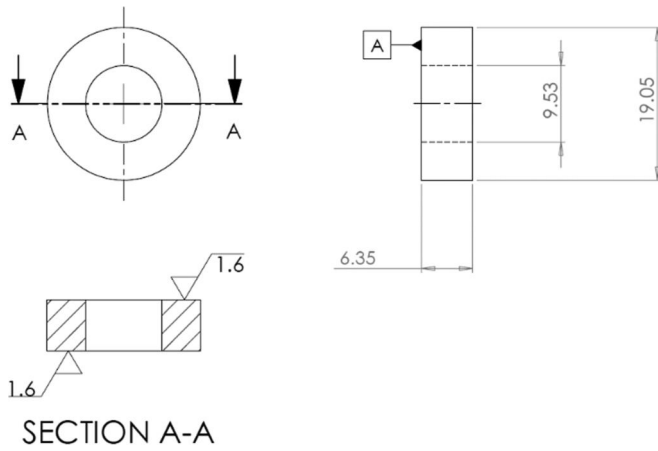


Figure 2. Ring compression test specimen drawing. All dimensions in mm and surface roughness (R_a) in μm .

50% (Fig. 1). Each load step was achieved at a constant velocity equivalent to a strain rate of 0.1 s^{-1} . While the actual strain rate will have deviated slightly during each load step (due to the changing height of the specimen), this approach was able to effectively eliminate strain rate as a variable across all of the test runs.

Variation in specimen diameter

The inner diameter of a specimen may take on a noncircular shape after deformation, especially if there is any degree of anisotropic frictional or material behavior, and therefore an averaged value for the inner diameter can be taken to account for this behavior (10). To measure for any anisotropic behavior, a sweep of the inner diameter was taken for each sample at every test load to obtain the maximum and minimum diameter. It was found across all load conditions that the variance of the average inner diameter was greater than the average variance between the maximum and minimum diameter typically by a factor no less than three. An example of the ovality of the test specimens at a load of 50 kN is shown in Fig. 3. It was therefore deemed appropriate to take an average of the maximum and minimum inner diameter when calculating the change in inner diameter because of the small measure of anisotropic behavior relative to the variance between test specimens.

Barreling compensation

Friction at the interface between the die and test specimen will result in barreling and an inhomogeneous strain field as the specimen is compressed (19). This creates a condition where the uniaxial stress state principle no longer holds true. Similar to Bridgman's correction factor (33), a bulge correction factor (C_f) was used to calculate the true stress (σ) of the ring specimens (34) at each load increment:

$$\sigma = C_f \frac{4P}{\pi(D^2 - d^2)} \quad [1]$$

where P is the compressive load, D is the outer diameter, and d is the inner diameter.

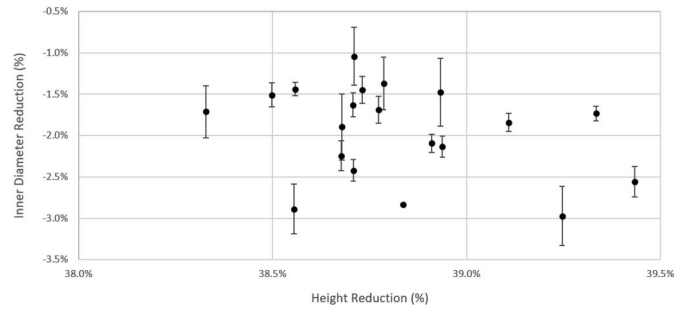


Figure 3. Variation of the inner diameter reduction percentage caused by the ovality of the test specimens for the 50 kN load condition. Larger error bars represent greater ovality.

The bulge correction factor is derived analytically from the analysis of the stress distribution at the midplane (35) and is given as

$$C_f = \left[\left(1 - \frac{2R}{a} \right) \ln \left(1 - \frac{a}{2R} \right) \right]^{-1} \quad [2]$$

where R is the outer bulge radius of the sample in the vertical plane and a is the outer radius at the horizontal midplane of the specimen. From geometric relations, the bulge radius was calculated as

$$R = \frac{h^2 + (D - d)}{4(D - d)} \quad [3]$$

where h is the actual height of the test specimen.

Finite-element simulation

Finite-element model

The computational model created to simulate the ring compression tests was made using the simulation software ANSYS. Due to the symmetric nature of the tests, an axisymmetric analysis was used to increase computational efficiency, with convergence achieved at 1734 nodes and 1579 elements. The flow stress model for AMS5643 followed a modified Hollomon profile and is given as

$$\sigma_{(MPa)} = 1526 \dot{\epsilon}^{-0.0198} \bar{\epsilon}^{(0.0528 \dot{\epsilon}^{-0.1398})} \quad [4]$$

where $\dot{\epsilon}$ is the true strain rate and $\bar{\epsilon}$ is the true strain. The upper and lower platens were modeled as rigid bodies, as is typical for bulk-metal models (10, 20).

Friction model

Friction is typically characterized by two models: either Coulomb's law or the Tresca friction model. For Coulomb's law, the tangential frictional stress is expressed as a function of the normal contact pressure and is given as

$$\tau_f = \mu \sigma_N \quad [5]$$

where τ_f is the tangential frictional stress, σ_N is the normal contact pressure, and μ is the coefficient of friction. A constant value for the coefficient of friction is only valid provided the ratio between the normal contact pressure and the

yield stress remains below approximately 1.3–1.5 (22, 35). Beyond this point, it is understood that the surface asperities at the contact interface will have deformed such that the real and apparent contact areas are equal. This leads to the frictional stress becoming constant and no longer proportional to the normal contact pressure, resulting in a decreasing coefficient of friction as the contact pressure increases. Under these conditions, the tangential frictional stress is better modeled by the Tresca friction model and is given as

$$\tau_f = mk \quad [6]$$

where m is the friction factor and k the materials shear strength. However, it has been shown that neither friction model can accurately reflect the dynamic friction conditions present in bulk-metal forming and that a hybrid between the two models is required (22).

The reference friction model used within ANSYS follows Coulomb's law and was used to create the FCCs.

Analysis and discussion

FCC interpolation

The conventional approach to determining the coefficient of friction from ring compression tests is as follows. The ring compression test is simulated in a computational model across a range of friction coefficients (for this study the required range required was 0.05–0.1). From these simulations, the results history for the percentage reduction in inner diameter is plotted against the percentage reduction in height to create the FCCs. Finally, the experiment ring compression data are compared to the simulated results and the coefficient of friction is determined by interpolating between the constant friction curves. The results of the FCC interpolation approach are shown in Fig. 4. By interpolating between the FCCs and calculating the average forming pressure at each load step, the pressure–friction relationship was determined and plotted in Fig. 5.

By running a custom command within the ANSYS simulation environment, the friction coefficient determined in Fig. 5 could be programmed into the computational model. As shown in Fig. 6, this custom friction model was able to produce a good prediction for the ring compression experiment data up to approximately a 30% height reduction, after which the computational model begins to underpredict the reduction in inner diameter. At a height reduction of 33.5%, the friction coefficient is evaluated to be 0.08 but the gradient of the experiment data is significantly steeper than the 0.08 constant friction curve (Fig. 7). It is clear to see that the friction coefficient should be greater than 0.08 to maintain the gradient of the experiment data and reach the next data point at 38.8%.

Iterative FCC

To improve on the FCC interpolation method, an iterative approach to generating the FCCs was proposed (Fig. 8) and is described as follows. First, constant friction curves were

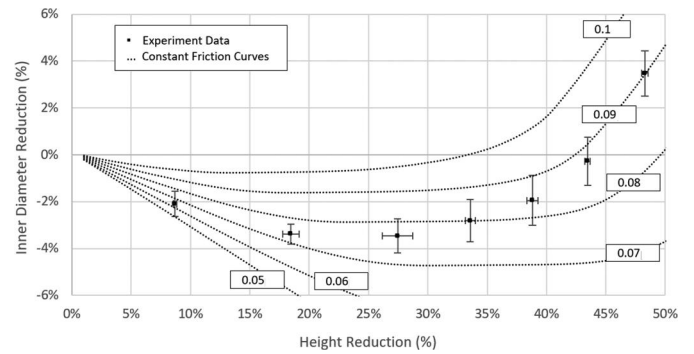


Figure 4. Ring compression test data for AMS5643 with a G-n Plus lubricant and FCCs ranging from a coefficient of friction of 0.05 to 0.1. Experiment error bars represent a 95% confidence interval.

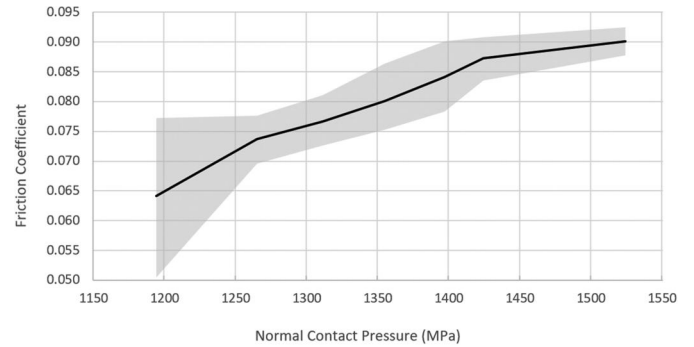


Figure 5. Variation in the coefficient of friction against contact pressure for steel AMS5643 with a G-n Plus lubricant. Shaded region, 95% confidence interval for the friction coefficient.

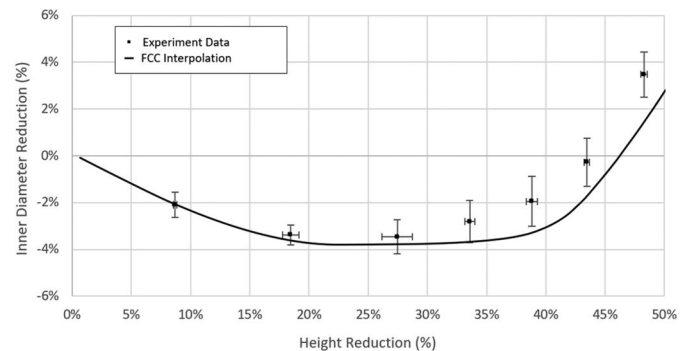


Figure 6. Comparison of the ring compression test data and the prediction using the FCC interpolation method.

created from the initial geometry up to the change in height recorded at the end of the first load step and the friction coefficient was evaluated similarly to the interpolation method. New constant friction curves were then generated starting from the geometry at the end of the first load to the end of the second load step and the friction coefficient was again evaluated for this second load step.

This is repeated across all load steps to produce a relationship between the contact pressure and the coefficient of friction. Figure 9 shows the results of this method. Because the friction coefficient was modeled as a constant throughout each load step, a final “smoothed” pressure–friction relationship was obtained by using the average pressure for each load step as shown in Fig. 9.

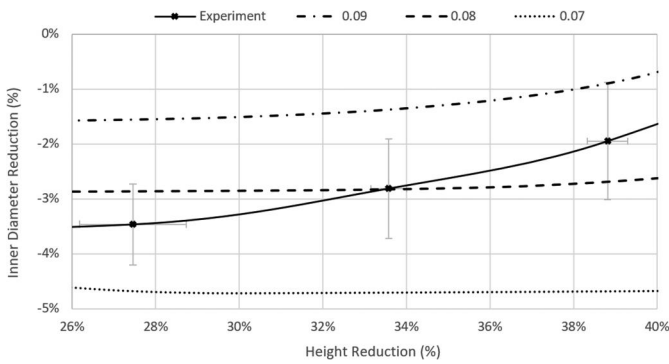


Figure 7. Detailed view from the FCCs in Fig. 3.

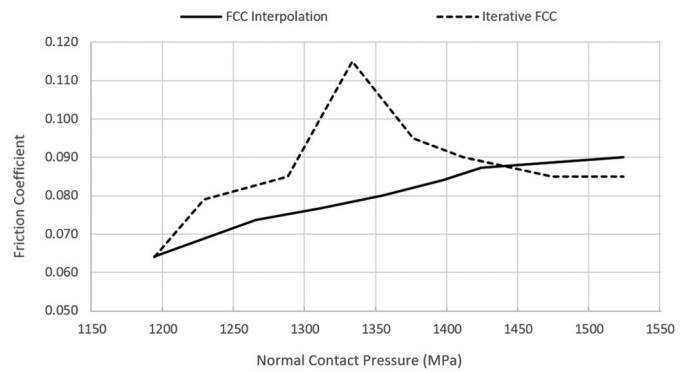


Figure 11. Friction–pressure relationship comparison.

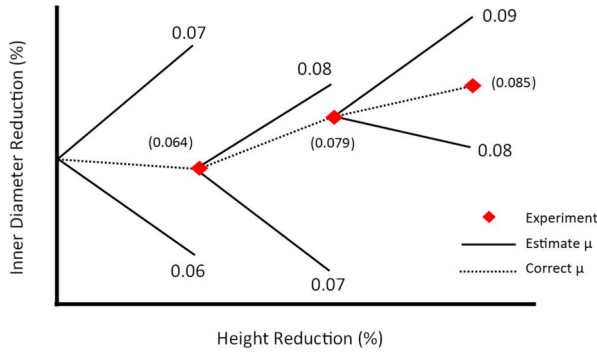


Figure 8. Schematic for the Iterative FCC methodology to evaluate the coefficient of friction (μ).

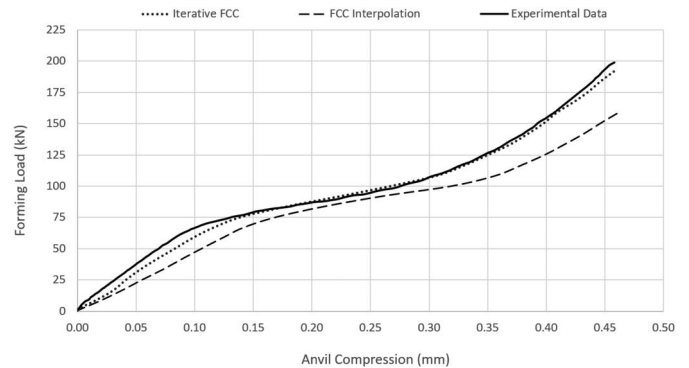


Figure 12. Performance of the two ring compression analysis methods compared to the forming loads experienced during the staking of a production spherical-plain bearing.

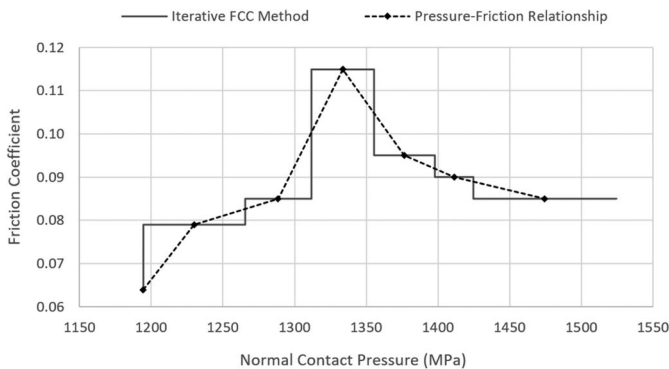


Figure 9. Pressure–friction relationship derived via the iterative FCC method.

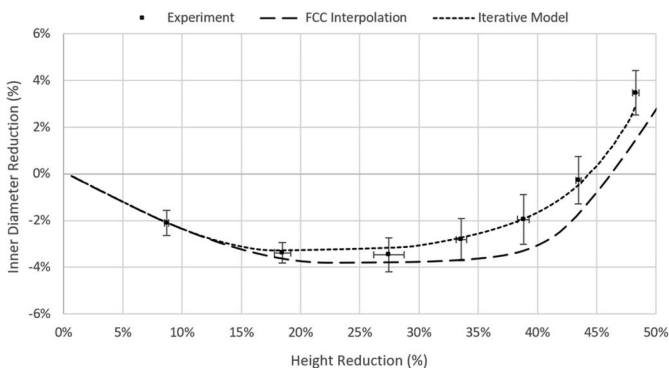


Figure 10. Comparison of the interpolation and iterative friction models to the ring compression experiment data.

When compared to FCC interpolation, the iterative FCC method produces a better prediction for the ring compression test and remains within the 95% confidence interval of

the experiment data across its entire test range (Fig. 10). A comparison of both contact pressure–coefficient of friction relationships is shown in Fig. 11.

The relationship generated by the iterative FCC method saw a rise in the friction coefficient from 0.064 to 0.115 at a contact pressure of 1334 MPa before decreasing to 0.085. The initial rise in the friction coefficient is likely attributed to the breakdown of the lubricant as the load-bearing capacity is exceeded and is spread thinner as the surface area of the test specimens increases with forming load. The peak friction coefficient at 1334 MPa was 1.35 times the yield strength of AMS5643 at 0.1 s^{-1} (985 MPa). This result agrees with the predicted decrease in friction coefficient expected at 1.3–1.5 times the yield strength (22, 36).

When viewed in a broader context, the significant improvements of the iterative-FCC method does not completely diminish the usefulness of the standard interpolation method if the coefficient of friction remains constant across the entire contact pressure range. Under these specific conditions the interpolation method can still produce accurate results without the need for further computational modeling. However, small changes in the evolution of the coefficient of friction can have a significant impact on the forming loads experienced during a forging process. To demonstrate this, a finite-element simulation was created to model the staking of a spherical-plain bearing (31) using the pressure–friction relationships derived from both analysis methods. As shown in Fig. 12, the iterative-FCC model was able to better predict the forming load across all ranges of anvil compression.

At a peak anvil compression of 0.46 mm, the error in the forming load of the interpolation method was $\sim 30\%$, compared to only $\sim 5\%$ for the iterative-FCC method.

Conclusions

Friction is one of the most important properties in metal forming operations, yet it is often neglected or simplified to a single constant value. Presented in this research is the evaluation of two different methods for determining the relationship between the contact pressure and coefficient of friction for steel AMS5643 via ring compression testing. The conventional method (FCC interpolation) compares the deformation of the ring specimens against FCCs simulating the ring compression test at various constant friction coefficients. The new method proposed in this study (iterative FCC) generates new FCCs for each load step that begins at the geometry of the last load step. The results from this research are summarized as follows:

- The FCC interpolation method provides a good initial prediction of the experimental data but fails to follow the experiment data at height reductions greater than 30%. Interpolation between FCCs is not able to describe the changing friction coefficient at each load step and becomes less accurate as the coefficient of friction changes more.
- The iterative FCC method was able to produce an accurate prediction of the experiment data, remaining within the 95% confidence interval across the entire test range.
- The iterative FCC coefficient of friction decreased from its maximum value of 0.115 after exceeding a contact pressure of 1334 MPa. This matched the theoretical decrease in the coefficient of friction expected at 1.3 to 1.5 times the yield strength of AMS5643.

The iterative FCC analysis method developed in this research can be applied to any ring compression test condition and provides improvement over the conventional FCC interpolation method. This improvement is expected to increase in conditions with higher contact pressures or when the variability of the coefficient of friction increases.

Acknowledgements

This research was conducted as part of the UWE 50/50 studentship scheme and with the support of SKF.

Conflicts of interest

The authors declare no conflicts of interest.

Disclosure statement

No potential conflict of interest was reported by the author(s).

ORCID

Jason Matthews  <http://orcid.org/0000-0002-4894-9309>

References

- (1) Kobayashi, S., Altan, T., and Oh, S. I. (1989), *Metal Forming and the Finite Element Method*, 4th ed., Oxford University Press: Oxford.
- (2) Sofuoglu, H., and Rasty, J. (1999), "On the Measurement of Friction Coefficient Utilizing the Ring Compression Test," *Journal of Engineering Materials and Technology*, **123**(3), pp 338–348. [10.1115/1.1369601](https://doi.org/10.1115/1.1369601)
- (3) Sedlacek, M., Gregorcic, P., and Podgornik, B. (2017), "Use of the Roughness Parameters Ssk and Sku to Control Friction—A Method for Designing Surface Texturing," *Tribology Transactions*, **60**(2), pp 260–266. [10.1080/10402004.2016.1159358](https://doi.org/10.1080/10402004.2016.1159358)
- (4) Menezes, P. L., Kishore, , and Kailas, S. V. (2009), "Study of Friction and Transfer Layer Formation in Copper-Steel Tribo-System: Role of Surface Texture and Roughness Parameters," *Tribology Transactions*, **52**(5), pp 611–622. [10.1080/10402000902825754](https://doi.org/10.1080/10402000902825754)
- (5) Qin, W., Jin, X., Kirk, A., Shipway, P. H., and Sun, W. (2018), "Effects of Surface Roughness on Local Friction and Temperature Distributions in a Steel-on-Steel Fretting Contact," *Tribology International*, **120**(1), pp 350–357. [10.1016/j.triboint.2018.01.016](https://doi.org/10.1016/j.triboint.2018.01.016)
- (6) Cristino, V. A. M., Rosa, P. A. R., and Martins, P. A. F. (2011), "Surface Roughness and Material Strength of Tribo-Pairs in Ring Compression Tests," *Tribology International*, **44**(2), pp 134–143. [10.1016/j.triboint.2010.10.002](https://doi.org/10.1016/j.triboint.2010.10.002)
- (7) Tomota, T., Masuda, R., Kondoh, Y., Ohmori, T., and Yagi, K. (2021), "Modeling Solid Contact between Rough Surfaces with Various Roughness Parameters," *Tribology Transactions*, **64**(1), pp 178–192. [10.1080/10402004.2020.1820123](https://doi.org/10.1080/10402004.2020.1820123)
- (8) He, X., Liu, Z., Ripley, L. B., Swensen, V. L., Griffin-Wiesner, I. J., Gulner, B. R., McAndrews, G. R., Weirser, J. R., Borovsky, B. P., Wang, Q. J., and Kim, S. H. (2021), "Empirical Relationship Between Interfacial Shear Stress and Contact Pressure in Micro- and Macro-Scale Friction," *Tribology International*, **155**, pp 1–8. [10.1016/j.triboint.2020.106780](https://doi.org/10.1016/j.triboint.2020.106780)
- (9) Fukagai, S., Marshall, M. B., and Lewis, R. (2022), "Transition of the Friction Behaviour and Contact Stiffness due to Repeated High-Pressure Contact and Slip," *Tribology International*, **170**, pp 1–14. [10.1016/j.triboint.2022.107487](https://doi.org/10.1016/j.triboint.2022.107487)
- (10) Woodhead, J., Truman, C. E., and Booker, J. D. (2015), "Modelling of Dynamic Friction in the Cold Forming of Plain Spherical Bearings," *Contact and Surface* 2015, Valencia, 21–23 April, pp 141–152. WIT Press: Southampton. [10.2495/SECM150131](https://doi.org/10.2495/SECM150131)
- (11) Hu, C., Chen, H., Zhang, W., and Ohshita, H. (2023), "Enhancing the Sensitivity of a Tribological Testing Method to Enable Development of Lubricants for Cold Forging," *Tribology International*, **179**, pp 1–10. [10.1016/j.triboint.2022.108156](https://doi.org/10.1016/j.triboint.2022.108156)
- (12) Pearson, S., Shipway, P. H., Aber, J. O., and Hewitt, R. A. A. (2013), "The Effect of Temperature on Wear and Friction of a High Strength Steel in Fretting," *Wear*, **303**(2), pp 622–631. [10.1016/j.wear.2013.03.048](https://doi.org/10.1016/j.wear.2013.03.048)
- (13) Zhu, K., Zeng, W., Ma, X., Tai, Q., Li, Z., and Li, X. (2011), "Determination of the Friction Factor of Ti-6Al-4V Titanium Alloy in Hot Forging by Means of Ring-Compression Test Using FEM," *Tribology International*, **44**(12), pp 2074–2080. [10.1016/j.triboint.2011.07.001](https://doi.org/10.1016/j.triboint.2011.07.001)
- (14) Mirahmadi, S. J., Hamed, M., and Cheraghzadeh, M. (2015), "Investigating Friction Factor in Forging of Ti-6Al-4V through Isothermal Ring Compression Test," *Tribology Transactions*, **58**, pp 778–785. [10.1080/10402004.2015.1019598](https://doi.org/10.1080/10402004.2015.1019598)
- (15) Kunogi, M. (1956), "A New Method of Cold Extrusion," *Journal of Scientific Research Institute*, **50**(1437), pp 215–246.

- (16) Male, A., and Cockcroft, M. G. (1964), "A Method for the Determination of the Coefficient of Friction of Metals Under Conditions of Bulk Plastic Deformation," *Journal of the Institute of Metals*, **93**(3), p 241.
- (17) Sofuoğlu, H., Gedikli, H., and Rasty, J. (2001), "Determination of Friction Coefficient by Employing the Ring Compression Test," *Journal of Engineering Materials and Technology, Transactions of the ASME*, **123**(3), pp 338–348 [10.1115/1.1369601](https://doi.org/10.1115/1.1369601)
- (18) Martin, F., Martin, M. J., Sevilla, L., and Sebastian, M. A. (2015), "The Ring Compression Test: Analysis of Dimensions and Canonical Geometry," *Procedia Engineering*, **132**(2015), pp 326–333. [10.1016/j.proeng.2015.12.502](https://doi.org/10.1016/j.proeng.2015.12.502)
- (19) Kahhal, P., Yeganehfar, M., and Kashfi, M. (2021), "An Experimental and Numerical Evaluation of Steel A105 Friction Coefficient Using Different Lubricants at High Temperature," *Tribology Transactions*, **65**(1), pp 25–31. [10.1080/10402004.2021.1966147](https://doi.org/10.1080/10402004.2021.1966147)
- (20) Kalpajian, S., and Schmid, S. R. (2008), *Manufacturing Processes for Engineering Materials*, 5th ed., Pearson Education: Canada.
- (21) Kobayashi, S. (1982), "A Review on the Finite-Element Method and Metal Forming Process Modeling," *Journal of Applied Metalworking*, **2**(1), pp 163–169. [10.1007/BF02834034](https://doi.org/10.1007/BF02834034)
- (22) Cora, Ö. N., Akkök, M., and Darendeliev, H. (2008), "Modelling of Variable Friction in Cold Forging," *Engineering Tribology*, **222**(1), pp 899–908. [10.1243/13506501JET419](https://doi.org/10.1243/13506501JET419)
- (23) Orsolini, A., and Booker, J. D. (2012), "Modelling Capabilities Required for the Double Nosing Process in the Assembly of Spherical Plain Bearings," *Journal of Engineering Manufacture*, **226**(5), pp 930–940. [10.1177/0954405411434679](https://doi.org/10.1177/0954405411434679)
- (24) Han, H. (2002), *Determination of Flow Stress and Coefficient of Friction for Extruded Anisotropic Materials under Cold Forming Conditions*, Royal Institute of Technology: Stockholm.
- (25) Lu, Y. (2005), "Study of Preform and Loading Rate in the Tube Nosing Process by Spherical Die," *Journal of Computational Methods in Applied Mechanics and Engineering*, **194**(25–26), pp 2839–2858. [10.1016/j.cma.2004.07.032](https://doi.org/10.1016/j.cma.2004.07.032)
- (26) Foster, A. D., Copeland, T. J., Cox, C. J., Hall, P. W., Watkins, M. A., Wright, R., and Lin, J. (2009), "Error Analysis and Correction in the Slab Method for Determining Forming Forces," *International Journal of Mechanical Education*, **37**(4), pp 304–317. [10.7227/IJMEE.37.4.4](https://doi.org/10.7227/IJMEE.37.4.4)
- (27) Gisbert, C., Bernal, C., and Camacho, A. M. (2015), "Improved Analytical Model for the Calculation of Forging Forces During Compression of Bimetallic Axial Assemblies," *Procedia Engineering*, **132**, pp 298–305. [10.1016/j.proeng.2015.12.498](https://doi.org/10.1016/j.proeng.2015.12.498)
- (28) Buschhausen, A., Weinmann, K., Altan, T., and Lee, J. (1992), "Evaluation of Lubrication and Friction in Cold Forging Using a Double Backward-Extrusion Process," *Journal of Material Processing Technology*, **33**(2), pp 95–108. [10.1016/0924-0136\(92\)90313-H](https://doi.org/10.1016/0924-0136(92)90313-H)
- (29) Kraus, M., Lenzen, M., and Markli, M. (2021), "Contact Pressure-Dependent Friction Characterization by Using a Single Sheet Metal Compression Test," *Wear*, **476**(1). [10.1016/j.wear.2021.203679](https://doi.org/10.1016/j.wear.2021.203679)
- (30) Bialas, M., Maciejewski, J., and Kucharski, S. (2021), "Friction Coefficient of Solid Lubricating Coating as a Function of Contact Pressure: Experimental Results and Microscale Modeling," *Continuum Mechanics and Thermodynamics*, **33**(1), pp 1733–1745. [10.1007/s00161-021-00999-0](https://doi.org/10.1007/s00161-021-00999-0)
- (31) Hatherell, J., Arnaud, M., Dennis, G., Curry, W., and Matthews, J. (2023), "Exploring the Potential for a FEA-Based Design of Experiments to Develop Design Tools for Bulk-Metal Joining Processes," *International Conference on Engineering Design (ICED)*, Bordeaux, France, 24–28 July.
- (32) Sofuoğlu, H., and Gedikli, H. (2002), "Determination of Friction Coefficient Encountered in Large Deformation Processes," *Tribology International*, **35**(1), pp 27–34. [10.1016/S0301-679X\(01\)00076-7](https://doi.org/10.1016/S0301-679X(01)00076-7)
- (33) Bridgman, P. W. (1952), *Studies in Large Plastic Flow and Fracture*, McGraw-Hill: New York.
- (34) Ettouney, O., and Hardt, D. E. (1983), "A Method for In-Process Failure Prediction in Cold Upset Forging," *ASME Journal of Manufacturing Science and Engineering*, **105**(1), pp 161–167. [10.1115/1.3185883](https://doi.org/10.1115/1.3185883)
- (35) Mielnik, E. M. (1991), *Metalworking Science and Engineering*, McGraw-Hill: New York.
- (36) Fereshteh-Saniee, F., Fallah-Nejad, K., Beheshtiha, A. S., and Badnava, H. (2013), "Investigation of Tension and Compression Behavior of AZ80 Magnesium Alloy," *Materials and Design*, **50**(1), pp 702–712. [10.1016/j.matdes.2013.03.080](https://doi.org/10.1016/j.matdes.2013.03.080)